HHS Public Access

Author manuscript

Tetrahedron. Author manuscript; available in PMC 2024 July 17.

Published in final edited form as:

Tetrahedron. 2023 July 17; 141: . doi:10.1016/j.tet.2023.133498.

Progress Toward the Asymmetric de Novo Synthesis of Lanostanes: A Counter Biomimetic Cucurbitane-to-Lanostane Type Transformation

Andrea R. Bucknam,

Glenn C. Micalizio*

Department of Chemistry, Dartmouth College, Burke Laboratory, Hanover, NH 03755, United States

Abstract

An oxidative rearrangement has been established that enables a cucurbitane-to-lanostane type rearrangement that is counter to known biomimetic transformations that proceed in an opposite direction by way of a lanostane-to-cucurbitane transformation. Here, an oxidative dearomatization/Wagner–Meerwein rearrangement with a substrate bearing the characteristic cucurbitane triad of quaternary centers at C9, C13 and C14, and possessing an alkene at C11–C12, proceeds in a manner that selectively shifts the methyl group at C9 to C10 in concert with the establishment of a sterically hindered allylic cation. The major product isolated from this transformation is formed by trapping of the allylic cation by addition of acetate to C12, rather than termination of the cascade by loss of a proton at C8. While proceeding by way of a unique sequence of bond-forming reactions that begins by oxidative dearomatization, this process achieves what we believe is an unprecedented cucurbitane-to-lanostane transformation, generating a product that contains the characteristic lantostane triad of quaternary centers at C10, C13 and C14 while also delivering a functionalized C-ring.

Graphical Abstract

*Corresponding Author glenn.c.micalizio@dartmouth.edu.

Declaration of competing interest

The authors declare the following financial interests/personal relationships which may be considered potential competing interests: Glenn C. Micalizio reports financial support was provided by the National Institutes of Health.

Appendix A. Supplementary data

Supplementary information related to this article can be found online at https://doi.org/10.101016/j.tet.##########.

The authors do not have any financial interest or personal relationships that may be perceived as influencing their work.

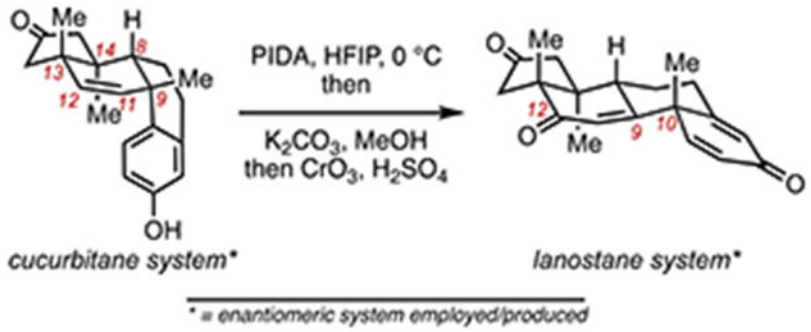

Keywords

Total synthesis; lanostane; cuciirbitane; oxidative dearomatization; Wagner–Meerwein rearrangement; tandem reaction

1. Introduction

Tetracyclic triterpenoids have attracted the attention of chemists and biologists for over a century. From early studies in structure elucidation to decades of investigations into their biosynthesis and countless campaigns in de novo synthesis, natural products in this broad structural class have had a profound impact on modern chemical and biological sciences. While numerous approaches to the asymmetric construction of estranes, androstanes, and pregnanes have appeared, more complex lanostane[1] and cucurbitane[2] systems present more challenging problems that have not been easy to address through de novo synthesis. As such, medicinally-focused pursuits based on these natural product classes have relied on natural product derivatization (or “semi-synthesis”) – an approach that comes with inherent molecular limitations based on the structures of the natural product starting materials available to fuel such programs.[3,4] As illustrated in Figure 1A, the general skeletons of lanostanes and cucurbitanes contain at least three stereodefined quaternary centers in their tetracyclic backbone, two of which are vicinal (at C13 and C14). While related, lanostanes and cucurbitanes have rather distinct molecular structures due to the differential placement of a stereodefined quaternary center at either C10 (lanostanes) or C9 (cucurbitanes). Despite decades of scientific inquiry into the biosynthesis of lanosterol, cholesterol, and steroid hormones, and the development of powerful biomimetic cation–olefin cyclization reactions, few successes have been reported for the de novo asymmetric synthesis of these more complex members of the tetracyclic triterpenoid family.[5] In fact, to date three syntheses of lanostane natural products have been reported, beginning with the landmark synthesis of lanosterol (**1**; Figure 1B) from cholesterol reported by Woodward in 1957.[6] Since then, a synthesis of lanostenol (**2**) from vitamin D was reported by Corey in 1994, and a de novo asymmetric synthesis of fomitellic acid B (**3**) was reported by Kobayashi in 2009.[7] As for cucurbitanes, we reported the first and, to our knowledge, the only asymmetric synthesis of any member of this class, octanorcucurbitacin B (**4**), in 2022.[8] Indeed, lanostane and cucurbitane natural products continue to stand as complex targets for modern asymmetric synthesis. In ongoing studies aimed at reimaging the manner in

which tetracyclic triterpenoid targets can be prepared synthetically we report here a new stereoselective entry to the lanostane system which embraces the reactivity of a complex cucurbitane-like intermediate recently encountered in our reported synthesis of **4**.

Lanostanes and cucurbitanes are biosynthetically related, as each is derived from 2,3-oxidosqualene (**I**) by way of the protosterol cation (**II**) (Figure 2A).[9] In this way, nature has revealed a divergent pathway for the construction of these natural product families that is based on how the protosterol cation (**II**) undergoes rearrangement. As depicted in Figure 2B, cationic rearrangement by way of a sequence of hydride and methyl shifts is terminated by loss of a proton at C9, delivering direct access to lanosterol (**1**). In the biosynthesis of cucurbitanes, a related sequence of hydride and methyl shifts is terminated by a hydride shift from C9 to deliver the cationic intermediate (**III**). Subsequent methyl shift from C10 to C9 occurs with hydride shift from C5 and loss of a proton from C6 to furnish the cucurbitane system **5** (cucurbitadienol). In this way, the protosterol cation (**II**) is ushered through a sequence that is terminated by a lanostane-to-cucurbitane rearrangement.

Aspects of these biosynthetic transformations have appeared as features of synthetic approaches to both lanostanes and cucurbitanes. For example, as illustrated in Figure 2C, a key step in Corey's synthesis of lanostenol (**2**) features a Lewis acid-mediated cation–olefin cyclization that establishes the AB-ring system (**6** → **7**).[7] Similarly, biosynthetically inspired lanostane-to-cucurbitane rearrangements have been reported on intermediates derived from semisynthesis (e.g., **8** → **9**). [10]

Recently, we reported a de novo asymmetric synthesis of a lanostane system based on late-stage introduction of the C14 quaternary center.[11] As illustrated in Figure 3A, the polyunsaturated epoxy-pregnene **10** served as an effective substrate for semi-Pinacol rearrangement mediated by the action of BF_3•OEt_2. In this way, **10** was smoothly converted to the lanostane system **11** that possesses the typical triad of stereodefined quaternary centers at C10, C13 and C14. Unfortunately, these early studies did not lead to a successful total synthesis due to challenges associated with stereoselective reduction of the C5–C6 alkene.

In contrast to this semi-Pinacol-based late-stage introduction of the C14 quaternary center, it was imagined that intermediates that we recently exploited in the synthesis of octanorcucurbitacin B (**4**) might prove useful in campaigns that target the construction of lanostane systems. Specifically, it was imagined that the dissolving metal reduction of cyclopropyl ketone **12** (Figure 3B) may set the stage for establishment of a synthetic branch-point capable of establishing a path to *either* cucurbitane (**4**) or lanostane systems (e.g., **14**). The latter of these was imagined by way of a cucurtitane-to-lanostane transformation that would proceed in the opposite direction of the biosynthetic lanostane-to-cucurbitane transformation previously presented in Figure 2. If possible, such a branchpoint would provide a synthetic means to mimic the divergent nature of the biosynthetic pathway that enables conversion of epoxy squalene (**I**) to lanosterol (**1**) or cucurbitadienol (**5**) (Figure 2A) yet doing so in a manner that exploits a molecular transformation that is decidedly not biomimetic. Here, we describe studies that have led to the establishment of such

a transformation and report a new tandem oxidative dearomatization reaction and group selective Wagner–Meerwein rearrangement process.

2. Results and discussion

As depicted in Figure 4A, previous studies have established tandem oxidative dearomatization and group-selective Wagner–Meerwein rearrangement as a means to convert unsaturated estranes (**15**) to polyunsaturated androstanes (**17**), presumably by way of the cationic intermediate **16**.[12] Here, the rearrangement process is thought to be terminated by acetatemediated deprotonation at C15. Inspired by this precedent, it was imagined that the cucurbitane system **18** (Figure 4B), may serve as a viable substrate for a related oxidative dearomatization and group-selective Wagner–Meerwein rearrangement. [13] In this case, exposure to $PhI(OAc)_2$ was reasoned to have the potential to deliver the allylic cation **19**. In contrast to the fully substituted and sterically hindered cationic intermediate **16**, the allylic cation **19** is positionally distinct (spanning C9, C11 and C12) and significantly less substituted. It was imagined that **19**, unlike **16**, could then participate in one of two types of terminating events: (1) loss of the C8 proton to deliver the C-ring diene **20**, or (2) regioselective substitution by acetate at C12 to deliver **21**.

It was recognized that the intermediate proposed for this counter biomimetic cucurbitane-to-lanostane rearrangement, phenol **18**, might be readily accessible from cyclopropyl ketone **12**, an intermediate that we previously employed in our asymmetric total synthesis of octanorcucurbitacin B (**4**) (Figure 5). In short, **12** is accessible from enyne **22** by an initial three-step conversion to the tetracyclic carbocycle **23** that features a highly selective metallacycle-mediated annulative cross-coupling and intramolecular Heck reaction.[14] Tetracycle **23** can then be converted to cyclopropyl ketone **12** in five additional steps.

Disappointingly, while **12** proved to be a useful intermediate en route to octanorcucurbitacin B (**4**), this material had been consumed in the previously reported natural product total synthesis campaign. Fortunately, because of an ongoing project in our laboratory, we had substantial quantities of *ent*-**12** available to explore our hypothesis for accomplishing the previously discussed counter-biomimetic cucurbitane-tolanostane transformation. As depicted in Figure 5, cyclopropyl ketone *ent*-**12** was converted to the proposed key intermediate *ent*-**18** by initial dissolving metal reduction (Li^0, NH_3, THF/*t*-BuOH) that simultaneously reduces the aromatic A-ring and regioselectively opens the cyclopropane. [8] Rearomatization (DDQ, PhMe) was then followed by Jones oxidation of the C16 alcohol to furnish the corresponding ketone, and demethylation (BBr_3, DCM, 0 °C) of the C3 methyl ether. With *ent*-**18** in hand, attention was then directed toward exploring the feasibility of the planned cucurbitane-to-lanostane transformation.

Satisfyingly, *ent*-**18** was found to be a viable substrate for the targeted oxidative dearomatization and group selective Wagner–Meerwein rearrangement. As shown, exposure to $PhI(OAc)_2$ resulted in the formation of the rearranged product **21** (R = H or Ac) in 78% yield – a structure that possesses the characteristic triad of stereodefined quaternary centers at C10, C13 and C14 seen in lanostane systems. Notably, this variation of the oxidative rearrangement proceeded by a termination event that is distinct from that seen with

earlier substrates, avoiding an elimination process and preferentially proceeding through regioselective substitution of the presumed allylic cation intermediate (*ent*-**19**) at C12. The resulting mixture of stereoisomeric acetates was then converted to the tetracyclic triketone **24** through saponification (K_2CO_3, MeOH) and Jones oxidation. While not a focus of the current studies, this cucurbitane-to-lanostane rearrangement is envisioned as a potentially powerful transformation in the context of future campaigns in natural product total synthesis and programs aimed at the design/discovery of natural product-inspired agents of potential therapeutic relevance.

3. Conclusions

Overall, these studies establish a novel counter biomimetic cucurbitane-to-lanostane transformation that proceeds by a unique sequence of oxidative dearomatization, group selective Wagner–Meerwein rearrangement, and regioselective trapping of the resulting allylic cation with acetate. While, to our knowledge, this is the first time such a tandem process has been reported, this complex transformation defines a branchpoint in our previously established route to octanorcucurbitatcin B (**4**) that paves the way to functionalized lanostane systems. In the context of our broader program that is reimagining the manner in which modern synthetic chemistry can be leveraged to address challenges that persist in this broad area of natural product-focused science, we note that the divergency described here is reminiscent of the divergency central to the biosynthetic means by which lanostanes and cucurbitanes are produced in nature. Finally, it has not escaped our attention that numerous tetracyclic triterpenoid natural products and medicinally relevant analogues thereof contain functionalized C-rings within their complex tetracyclic skeletons, and new strategies to establish such systems in a direct and stereoselective fashion could be quite valuable.

4. Experimental section

4.1 Materials and methods

All reagents and starting materials were purchased from commercial sources and used as received, unless otherwise indicated. Anhydrous tetrahydrofuran (THF), dichloromethane (DCM) and toluene (PhMe) were obtained by passing HPLC grade solvents through a column of activated alumina using a Glass Contour Solvent Purification System by Pure Process Technology, LLC. For flash column chromatography, HPLC grade solvents were used without further purification. All reactions were conducted in flame-dried glassware under an atmosphere of dry nitrogen unless otherwise indicated. Reaction mixtures were magnetically stirred, and their progress was monitored by thin layer chromatography (TLC) on EMD TLC silica gel 60 F_{254} glass-backed plates. Compounds were visualized by initial exposure of TLC plates to UV-light (254 nm), followed by staining with *p*-anisaldehyde. Purification of crude isolates was achieved by flash column chromatography on a Biotage® Isolera One™ Automated Liquid Chromatography System using Biotage® Sfar Silica HC D 5–10 g silica gel cartridges. Concentration of reaction product solutions and chromatography fractions was accomplished by rotary evaporation at 30–35 °C under the appropriate pressure, followed by concentration at room temperature on a vacuum pump (approx. 0–1

mbar). Yields refer to chromatographically purified and spectroscopically pure compounds, unless otherwise indicated. ^{1}H-NMR data were recorded on a Bruker Avance III 500 MHz NMR spectrometer (TBI probe) and a Bruker Avance III 600 MHz spectrometer (BBFO probe). ^{1}H chemical shifts are reported in parts per million (ppm, δ scale) downfield from tetramethylsilane and are referenced to the residual protium in $CDCl_3$ (7.26 ppm). NMR coupling constants are measured in Hertz (Hz), and splitting patterns are indicated as follows: br, broad; s, singlet; d, doublet; t, triplet; q, quartet; m, multiplet. ^{13}C {1H decoupled} NMR data were recorded at 150 MHz on a Bruker Avance III 600 MHz spectrometer (BBFO probe). ^{13}C chemical shifts are reported in parts per million (ppm, δ scale) and are referenced to the central line of the carbon resonances of the solvent: $CDCl_3$ (77.16 ppm). Structural assignments for new compounds were supported by two-dimensional NMR experiments (COSY, HSQC, HMBC and NOESY) recorded on a Bruker Avance III 600 MHz spectrometer (BBFO probe). Infrared spectra were collected on a JASCO FT/IR-4100 Fourier Transform Infrared Spectrometer. HRMS (EI-TOF) analyses were performed at the Mass Spectrometry Laboratory of the University of Illinois at Urbana-Champaign. Optical rotations (α) were obtained on a JASCOP-2000 polarimeter equipped with tungsten-halogen lamp (WI) and interface filter set to 589 nm, using a sample cell with a pathlength of 100 nm. Specific rotations are reported as: $[\alpha]_{589}^{T(^{\circ}C)}$ (*c*, solvent) and are based on the equation $[\alpha]_{589}^{T(^{\circ}C)} = (100 \cdot \alpha)(l \cdot c)$, where the concentration (*c*) is reported as g/100 ml and the pathlength (*l*) in decimeters.

4.2 Experimental procedures

Enol ether S1.—A three-necked, 250-mL round bottom flask was equipped with a Dewar condenser. Ammonia gas was condensed (approx. 50 mL) into the round bottom flask at −78 °C, and then the flask was placed under nitrogen atmosphere. Lithium metal (0.31g, 44.94 mmol, 66 equiv) was added in one portion. The resulting dark blue solution was stirred for 15 minutes at −78 °C. Then, ent-**12** [ref.8] (0.210 g, 0.681 mmol, 1 equiv) was added in a 1:1 solution of THF/t-BuOH (25 mL total, prepared from 12.5 mL THF and 12.5 mL t-BuOH). The dark blue solution was stirred for 1 hour at −78 °C, then was allowed to warm to room temperature and was stirred for an additional 1 hour, maintaining the −78 °C Dewar condenser above the reaction flask the entire time. The solution was then returned to −78 °C and ~20 mL of a saturated aqueous solution of NH_4Cl was added, slowly. When the entire solution had changed in appearance from dark blue to clear, it was allowed to warm to room temperature. The ammonia was allowed to evaporate under a stream of nitrogen gas. The solution was then diluted with DCM (~50 mL) and DI water (~50 mL). The organic layer was separated, and the aqueous layer was extracted with DCM (5 x 50 mL). The combined organic layers were dried over Na_2SO_4, filtered through Celite, and concentrated in vacuo. The crude product was purified by flash column chromatography on a Biotage® Sfar Silica HC D 10 g cartridge with 93:7 to 40:60 hexanes–ethyl acetate gradient elution to afford the tentatively assigned diastereomeric mixture of enol ether **S1** (0.159 g, 74%) as a clear oil.

Diastereomeric mixture of enol ether **S1**: ^{1}H NMR (600 MHz, $CDCl_3$) and ^{13}C NMR (151 MHz, $CDCl_3$) are reported in Supporting Information Section 5, “NMR Spectra. ” TLC (SiO_2) R_F = 0.4 (30% EtOAc/Hexanes). IR (Thin film, cm^{-1}) 3790, 3662, 2954, 2927, 1218. HRMS (ESI-TOF) m/z: [M+H]+ Calculated for $C_{21}H_{31}O_2$ 315.2324; found 315.2313.

Alcohol S2.—To a 25-mL round bottom flask equipped with stir bar was added enol ether **S1** (79.0 mg, 0.251 mmol, 1 equiv) in PhMe (5 mL). To this solution was added 2,3-dichloro-5,6-dicyano-1,4-benzoquinone (0.120 g, 0.528 mmol, 2.1 equiv) in one portion. The resulting red solution was allowed to stir at room temperature for 3.5 hours, monitored by TLC. Upon completion as determined by TLC analysis, the solution was concentrated under reduced pressure to give a dark red residue which was purified by flash column chromatography on a Biotage® Sfar Silica HC D 5 g cartridge with 93:7 to 40:60 hexanes–ethyl acetate gradient elution to afford the tentatively assigned diastereomeric mixture of alcohol **S2** (58.9 mg, 75%) as a white foam. Alcohol **S2**: ^{1}H NMR (600 MHz, $CDCl_3$) and ^{13}C NMR (151 MHz, $CDCl_3$) are reported in Section 5, "NMR Spectra. " TLC (SiO_2) R_F = 0.4 (40% EtOAc/Hexanes). IR (Thin film, cm^{-1}) 3371, 2947, 1605, 1255. HRMS (ESI-TOF) m/z: [M+H]+ Calculated for $C_{21}H_{29}O_2$ 313.2168; found 313.2154.

Ketone S3.—To prepare the Jones reagent (CrO_3/H_2SO_4, ~3.8 M in H_2O): In a 10-mL round bottom flask with stir bar, chromium (IV) oxide (0.167 g) was dissolved in DI H_2O (0.31 mL) at room temperature. To this solution was added concentrated sulfuric acid (0.15 mL), slowly. An additional 0.13 mL DI H_2O was added to dissolve insoluble salts, resulting in a red solution. In a separate 50-mL round bottom flask, a solution of alcohol **S2** (48.0 mg, 0.156 mmol, 1 equiv) in acetone (16 mL) was allowed to stir at room temperature and the freshly prepared Jones reagent (81 μL, 0.311 mmol, 2 equiv) was added dropwise. The green solution was allowed to stir 30 minutes at room temperature. Upon completion as determined by TLC analysis, iPrOH (1.2 mL) was added to quench remaining oxidant. The solvent was removed in vacuo. The resulting green residue was diluted with H_2O (25 mL) and EtOAc (25 mL), and the organic layer was separated. The aqueous layer was extracted with EtOAc (3 x 25 mL). The combined organic layers were dried over $MgSO_4$, filtered, and concentrated in vacuo to give ketone **S3** (41.0 mg, 85%) as an orange residue, which was used without further purification. **S3**: TLC (SiO_2) R_F = 0.8 (30% EtOAc/Hexanes). Specific Rotation $[\alpha]_{589}^{20.4} = +172.2$ (*c* 0.25, $CHCl_3$). ^{1}H NMR (600MHz, $CDCl_3$) δ 7.28 (d, J = 8.6 Hz, 1H), 6.72 (dd, J = 8.6, 2.5 Hz, 1H), 6.67 (d, J = 2.1 Hz, 1H), 6.17 (d, J = 10.0 Hz, 1H), 5.96 (d, J = 9.9 Hz, 1H), 3.78 (s, 3H), 2.86 (ddd, J = 16.0, 10.7, 5.5 Hz, 1H), 2.74 (dt, J = 15.5, 5.3 Hz, 1H), 2.63 (t, J = 7.8 Hz, 1H), 2.51 (d, J = 17.8 Hz, 1H), 2.29 (d, J = 17.4 Hz, 1H), 2.16 – 2.06 (m, 1H), 1.98 (dd, J = 17.5, 6.6 Hz, 2H), 1.58 – 1.49 (m, 1H), 1.32 (s, 3H), 1.21 (s, 3H), 0.69 (s, 3H). ^{13}C NMR (151 MHz, $CDCl_3$) δ 218.86, 157.22, 139.39, 137.08, 134.85, 130.47, 125.31, 114.11, 111.81, 55.24, 48.74, 48.35, 45.35, 44.79, 43.01, 39.46, 33.46, 28.69, 27.04, 24.02, 19.74. IR (Thin film, cm^{-1}) 2954, 1741, 1609. HRMS (ESI-TOF) m/z: [M+H]+ Calculated for $C_{21}H_{27}O_2$ 311.2011, found 311.2003.

ent-Phenol 18.—Ketone **S3** (34 mg, 0.112 mmol, 1 equiv) was dissolved in DCM (11 mL) and the solution was cooled to 0 °C. Boron tribromide (33 μL, 0.335 mmol, 3 equiv) was added dropwise. The solution was allowed to stir 2.5 hours at 0 °C, progress monitored by TLC. Upon consumption of the starting material as determined by TLC analysis, MeOH (10 mL) was added to quench. The solution was poured over a cold saturated aqueous $NaHCO_3$ solution (25 mL). The organic layer was separated and the aqueous layer was extracted with DCM (3 x 25 mL). Combined organic layers were dried over $MgSO_4$, filtered, and concentrated in vacuo. The crude product was purified by flash column chromatography on

a Biotage® Sfar Silica HC D 5 g cartridge with 93:7 to 40:60 hexanes–ethyl acetate gradient elution to afford ent-phenol **18** (29 mg, 89%) as a clear oil. **ent-Phenol 18**: TLC (SiO_2) R_F = 0.5 (30% EtOAc/Hexanes). Specific Rotation $[\alpha]_{589}^{20.5} = +72.2$ (*c* 0.25, $CHCl_3$). ^{1}H NMR (600 MHz, $CDCl_3$) δ 7.21 (d, J = 8.4 Hz, 1H), 6.65 (dd, J = 8.4, 2.6 Hz, 1H), 6.61 (d, J = 2.2 Hz, 1H), 6.15 (d, J = 10.0 Hz, 1H), 5.95 (d, J = 10.0 Hz, 1H), 5.19 (s, 1H), 2.82 (ddd, J = 16.0, 10.9, 5.6 Hz, 1H), 2.69 (dt, J = 15.5, 5.3 Hz, 1H), 2.62 (t, J = 7.9 Hz, 1H), 2.51 (d, J = 17.9 Hz, 1H), 2.29 (d, J = 17.4 Hz, 1H), 2.09 (td, J = 13.7, 5.5 Hz, 1H), 1.99 (dd, J = 17.5, 12.3 Hz, 2H), 1.50 (tt, J = 13.2, 6.5 Hz, 1H), 1.31 (s, 3H), 1.20 (s, 3H), 0.66 (s, 3H). ^{13}C NMR (151 MHz, $CDCl_3$) δ 219.46, 153.25, 139.69, 137.14, 134.86, 130.44, 125.51, 115.53, 113.39, 48.77, 48.38, 45.37, 44.80, 42.98, 39.48, 33.44, 28.50, 27.05, 23.97, 19.72. IR (Thin film, cm^{-1}) 3376, 2954, 1730. HRMS (ESI-TOF) m/z: [M+H]+ Calculated for $C_{20}H_{25}O_2$ 297.1849; found 297.1855. Analysis of relative stereochemistry: HSQC, COSY and HMBC experiments were used to assign all ^{1}H NMR signals for ent-phenol **18**, and 1D NOESY experiments revealed the correlations shown in Supporting Information Section 5: NMR Spectra, allowing relative stereochemistry to be assigned.

ent*-lanostane-based dienones 21a and 21b.—ent*-Phenol **18** (20 mg, 0.068 mmol, 1 equiv) was dissolved in HFIP (2 mL) and the clear solution was cooled to 0 °C. PIDA (25 mg, 0.769 mmol, 1.1 equiv) was added in one portion and the resulting yellow solution was allowed to stir 1 minute. Then, a saturated aqueous solution of $NaHCO_3$ (2 mL) was added. HFIP was removed *in vacuo* and the remaining slurry was diluted with EtOAc (2 mL). The organic layer was separated and the aqueous layer was extracted with EtOAc (3 x 5 mL). The combined organic layers were dried over $MgSO_4$, filtered, and concentrated *in vacuo*. The crude residue was purified by pipet column silica gel chromatography from 100:0 to 70:30 hexanes–ethyl acetate gradient elution to afford both the *ent*-lanostane-based dienone **21a** (11 mg, 46%) and **21b** (7 mg, 32%) in a 78% combined yield, both products as clear oils. Diastereomeric mixture of **21a**: *^{1}H NMR (600 MHz, $CDCl_3$) and ^{13}C NMR (151 MHz, $CDCl_3$) are reported in* the Supporting Information Section 4, "NMR Spectra. " TLC (SiO_2) R_F = 0.3 (50% EtOAc/Hexanes). *IR (Thin film, cm^{-1}) 2961, 1739, 1661, 1631, 1240. HRMS (ESI-TOF) m/z: [M+H]+ Calculated for $C_{22}H_{27}O_4$ 355.1909; found 355.1905.* **21b**: TLC (SiO_2) R_F = 0.1 (50% EtOAc/Hexanes). *Specific Rotation* $[\alpha]_{589}^{20.6} = +36.9$ (*c 0.05 $CHCl_3$*). ^{1}H NMR (600 MHz, $CDCl_3$) δ 7.29 (d, *J* = 10.2 Hz, 1H), 6.31 (d, *J* = 11.7 Hz, 1H), 6.12 (s, 1H), 5.93 (d, *J* = 5.4 Hz, 1H), 3.98 (app. s, 1H), 2.94 (d, *J* = 18.2 Hz, 1H), 2.71 – 2.62 (m, 2 H), 2.53 – 2.44 (m, 1H), 2.36 (d, *J* = 17.7 Hz, 1H), 2.05 (d, *J* = 17.2 Hz, 1H), 1.91 (d, *J* = 18.2 Hz, 1H), 1.89 – 1.82 (m, 1H), 1.70 – 1.56 (m, 1H), 1.46 (s, 3H), 1.02 (s, 3H), 1.00 (s, 3H). ^{13}C NMR (151 MHz, $CDCl_3$) δ 217.58, 186.07, 165.38, 152.86, 145.90, 127.80, 124.51, 122.25, 71.74, 49.94, 45.72, 45.12, 44.84, 42.18, 40.77, 32.32, 30.20, 28.92, 22.61, 20.60. IR *(Thin film, cm^{-1}) 3418, 1735, 1658, 1616.* HRMS (ESI-TOF) m/z: [M+H]+ Calculated for $C_{20}H_{25}O_3$ 313.1804; found 313.1800. *Analysis of relative stereochemistry: HSQC, COSY and HMBC experiments were used to assign all ^{1}H NMR signals for* **21b**, *and* ID NOESY experiments revealed the correlations shown in Supporting Information Section 5: NMR Spectra, allowing relative stereochemistry to be assigned.

***ent*-lanostane-based trienone 24.—**The combined products **21a** and **21b** (0.050 mmol total, 1 equiv) were dissolved in a 1:1 solution of MeOH/THF (1.6 mL total) at room

temperature. Potassium carbonate (21 mg, 0.155 mmol, 5 equiv) was added in one portion and the mixture was allowed to stir at room temperature, progress monitored by TLC (5 hours). Upon consumption of starting material as judged by TLC analysis, to the reaction mixture was added a saturated aqueous NH_4Cl solution (0.5 mL). The solution was diluted with EtOAc (2 mL) and the organic layer was separated. The remaining aqueous solution was extracted with EtOAc (3 x 5 mL). The combined organic layers were allowed to dry over $MgSO_4$, filtered, and concentrated in vacuo. The crude residue was diluted in acetone (0.5 mL) at room temperature. In a separate flask, to prepare the Jones reagent (CrO_3/H_2SO_4, ~3.8 M in H_2O): In a 10-mL round bottom flask with stir bar, chromium (IV) oxide (56 mg) was dissolved in DI H_2O (100 μL) at room temperature. To this solution was added concentrated sulfuric acid (50 μL), slowly. An additional 40 μL DI H_2O was added to dissolve insoluble salts, resulting in a red solution. To the solution of the crude residue (from previous) in acetone was added the freshly prepared Jones reagent (26 μL. 0.100 mmol, 2 equiv). Reaction progress was monitored by TLC (15 minutes). Upon consumption of starting material, Jones' reagent was quenched by the addition of iPrOH (0.5 mL). The solvent was removed in vacuo and the red residue was diluted with EtOAc (10 mL) and water (10 mL). The organic layer was separated, and the aqueous layer was extracted with EtOAc (5 x 10 mL). The combined organic layers were dried over $MgSO_4$, filtered, and concentrated in vacuo. The crude residue was purified by pipet column silica gel chromatography from 100:0 to 60:40 hexanes–ethyl acetate gradient elution to afford **24** (8.4 mg, 50% over 2 steps) as a clear oil. **ent-Lanostane-based 24**: TLC (SiO_2) R_F = 0.2 (50% EtOAc/Hexanes). Specific Rotation $[\alpha]_{589}^{20.8} = +190.4$ (*c* 0.05, $CHCl_3$). ^{1}H NMR (600 MHz, $CDCl_3$) δ 7.20 (d, J = 10.2 Hz, 1H), 6.36 (dd, J = 10.2, 1.9 Hz, 1H), 6.19 (d, J = 1.7 Hz, 1H), 6.04 (d, J = 2.5 Hz, 1H), 3.10 (ddd, J = 12.9, 5.4, 2.6 Hz, 1H), 2.84 (d, J = 18.9 Hz, 1H), 2.78 (tdd, J = 13.7, 4.6, 1.6 Hz, 1H), 2.59 (dt, J = 13.5, 3.5 Hz, 1H), 2.51 (d, J = 17.3 Hz, 1H), 2.20 (d, J = 17.4 Hz, 1H), 2.10 – 2.02 (m, 1H), 2.00 – 1.94 (m, 1H), 1.72 (qd, J = 13.2, 4.1 Hz, 1H), 1.60 (s, 3H), 1.30 (s, 3H), 0.89 (d, J = 1.5 Hz, 3H). ^{13}C NMR (151 MHz, $CDCl_3$) δ 214.45, 200.60, 185.38, 162.85, 162.11, 150.75, 128.55, 125.62, 123.11, 53.45, 48.37, 45.92, 44.62, 43.81, 42.04, 31.86, 29.78, 29.09, 21.37, 18.54. IR (Thin film, cm^{-1}) 3052, 2986, 1741, 1686, 1668. HRMS (ESI-TOF) m/z: [M+H]+ Calculated for $C_{21}H_{29}O_2$ 311.1647; found 311.1647. Analysis of relative stereochemistry: HSQC, COSY and HMBC experiments were used to assign all ^{1}H NMR signals for **24**. See Supporting Information Section 5: NMR Spectra.

Supplementary Material

Refer to Web version on PubMed Central for supplementary material.

Acknowledgments

We gratefully acknowledge financial support of this work by the National Institutes of Health (NIGMS R35 GM134725).

Data Availability

No data was used for the research described in the article.

References

[1]. For a recent review, see: Yang Y-P; Tasneem S; Daniyal M; Zhang L; Jia Y-Z; Jian Y-Q; Li B; Wang W Lanostane Tetracyclic Triterpenoids as Important Sources for Anti-Inflammatory Drug Discovery. World J. Tradit. Chin. Med 2020, 6, 229.

[2]. For a review, see: Chen JC; Chiu MH; Nie RL; Cordell GA; Qiu SX Cucurbitacins and Cucurbitane Glycosides: Structures and Biological Activities. Nat. Prod. Rep 2005, 22, 386. [PubMed: 16010347]

[3]. (a)Kennedy EM; P'Pool SJ; Jiang J; Sliva D; Minto RE Semisynthesis and Biological Evaluation of Ganodermanontriol and Its Stereoisomeric Triols. J. Nat. Prod 2011, 74, 2332–2337. [PubMed: 22044278] (b)Ukiya M; Hayakawa T; Okazaki K; Hikawa M; Akazawa H; Li W; Koike K; Fukatsu M Synthesis of Lanostane-Type Triterpenoid N-Glycosides and Their Cytotoxicity against Human Cancer Cell Lines. Chem. Biodivers 2018, 15, No. el800113. (c)Chinthanom P; Vichai V; Dokladda K; Sappan M; Thongpan-chang T; Isaka M Semisynthetic Modifications of Antitubercular Lanostane Triterpenoids from Ganoderma. J. Antibiot 2021, 74, 435–442.(d)Kikuchi K; Ishii K; Ogihara E; Zhang J; Ukiya M; Tokuda H; Iida T; Tanaka R; Akihisa T Cytotoxic and Apoptosis-Inducing Activities, and Anti-Tumor-Promoting Effects of Cyanogenated and Oxygenated Triterpenes. Chem. Biodivers 2014, 11, 491–504. [PubMed: 24706621]

[4]. (a)Ramalhete C; Lopes D; Molnár J; Mulhovo S; Rosário VE; Ferreira M-JU Karavilagenin C derivatives as antimalarials. Bioorg. Med. Chem 2011, 19, 330–338. [PubMed: 21129980] (b)Lang KL; Silva IT; Zimmermann LA; Machado VR; Teixeira MR; Lapuh ML ; Galetti MA ; Palermo JA; Cabrera GM; Campos Bernardes LS; Oliveira Simões CM; Schenkel EP; Balparda Caro MS; Duran FJ Synthesis and cytotoxic activity evaluation of dihydrocucurbitacin B and cucurbitacin B derivatives. Bioorg. Med. Chem 2012, 20, 3016–3030. [PubMed: 22472043] (c)Guo R-H; Geng C-A; Huang X-Y; Ma Y-B; Zhang Q; Wang L-J; Zhang X-M; Zhang R-P; Chen J-J Synthesis of hemslecin A derivatives: A new class of hepatitis B virus inhibitors. Bioorg. Med. Chem. Lett 2013, 23, 1201–1205. [PubMed: 23385212] (d)Silva IT; Carvalho Z; Lang KL; Dudek SE; Masemann D; Durán FJ; Caro MSB; Rapp UF; Wixler V; Schenkel EP; Simões CMO; Ludwig S In Vitro and In Vivo Antitumor Activity of a Novel Semisynthetic Derivative of Cucurbitacin B. PLoSOne 2015,10, e0117794.(e)Ge W; Chen X; Han E; Liu Z; Wang T; Wang M; Chen Y; Ding Y; Zhang Q Synthesis of Cucurbitacin B Derivatives as Potential AntiHepatocellular Carcinoma Agents. Molecules 2018, 23, 3345. [PubMed: 30567327] (f)Wang J; Liu J; Xie Z; Li J; Li J; Hu L Design, synthesis and biological evaluation of mogrol derivatives as a novel class of AMPKa2b1g1 activators. Bioorg. Med. Chem. Lett 2020, 30, 126790. [PubMed: 31744674] (g)Yu K; Yang X; Li Y; Cui X; Liu B; Yao Q Synthesis of cucurbitacin IIa derivatives with apoptosis-inducing capabilities in human cancer cells. RSC Adv. 2020, 10, 3872–3881. [PubMed: 35492669] (h)Song J-R; Li N; Li D-P Synthesis and anti-proliferation activity of mogrol derivatives bearing quinoline and triazole moieties. Bioorg. Med. Chem. Lett 2021, 42, 128090. [PubMed: 33964443]

[5]. For a review, see: Yoder RA; Johnston JN A Case Study in Biomimetic Total Synthesis: Polyolefin Carbocyclizations to Terpenes and Steroids. Chem. Rev 2005,105, 4730–4756. [PubMed: 16351060]

[6]. For the conversion of cholesterol to lanosterol, see: Woodward RA, ; Patchett AA; Barton DHR; Ives DAJ; Kelly RB The Synthesis of Lanosterol (Lanostadienol). J. Chem. Soc 1957, 1131–1144.

[7]. For a synthesis of lanostenol from vitamin D, see: (a)Corey EJ; Lee J; Liu DR First Demonstration of a Carbocation–Olefin Cyclization Route to the Lanosterol Series. Tetrahedron Lett. 1994, 35, 9149–9152.For a *de novo* asymmetric synthesis of fomitillic acid B: (b) Yamaoka M; Nakazaki A; Kobayashi S Total synthesis of fomitellic acid B. Tetrahedron Lett. 2009, 50, 6764–6768.

[8]. Bucknam AR; Micalizio GC Asymmetric De Novo Synthesis of a Cucurbitane Triterpenoid: Total Synthesis of Octanorcucurbitacin B. J. Am. Chem. Soc 2022,144, 8493–8497. [PubMed: 35533213]

[9]. (a)Abe I; Rohmer M; Prestwich GD Enzymatic Cyclization of Squalene and Oxidosqalene to Sterols and Triterpenes. Chem. Rev 1993, 95, 2189–2206.(b)Corey EJ; Russey WE; de Montellano PRO 2,3-Oxidosqualene, an Intermediate in the Biological Synthesis of Sterols from

Squalene. J. Am. Chem. Soc. 1966, 88, 4750–4751 [PubMed: 5918046] (c)Shibuya M; Adachi S; Ebizuka Y Cucurbitadienol synthase, the first committed enzyme for cucurbitacin biosynthesis, is a distinct enzyme from cycloartenol synthase for phytosterol biosynthesis. Tetrahedron 2004, 60, 6995–7003.

[10]. For examples of lanostane-to-cucurbitane transformations, see: (a)Paryzek Z Tetracyclic Triterpenes. Part 2. A Synthetic Approach to Cucurbitacins. J. Chem. Soc. P.T.1 1979, 1222–1227.(b)Edwards OE; Paryzek Z Lanostane-to-cucurbitane transformation. Can. J. Chem 1983, 61, 1973–1980.(c)Paryzek Z; Wydra R Tetracyclic triterpenes. VIII. The skeletal rearrangement of 3β-acetaoxy-9α,11α-epoxy-5α-lanostan-7-one: 13- and 10-methyl group migration. Can. J. Chem 1985, 63, 1280–1286.(d)Edwards OE; Kolt RJ Lanostane to cucurbitane transformations. Can. J. Chem 1987, 65, 595–612.

[11]. Wai EL; Micalizio GC Toward the Asymmetric de Novo Synthesis of Lanostanes: Construction of 7,11-Dideoxy-Δ^5-Lucidadone H. J. Org. Chem 2022, 87, 14975–14979. [PubMed: 36206482]

[12]. For examples of oxidative dearomatization/Wagner-Meerwein rearrangements, see: (a)Kim WS; Shalit ZA; Nguyen SM; Schoepke E; Eastman A; Burris TP; Gaur AB; Micalizio GA A Synthesis Strategy for Tetracyclic Terpenoids Leads to Agonists of ERβ. Nat Commun 2019, 10, 2448. [PubMed: 31164645] (b)Shalit ZA; Valdes LC; Kim WS; Micalizio GC From an *ent*-Estrane, through a *nat*-Androstane, to the Total Synthesis of the Marine-Derived $\Delta^{8,9}$-Pregnene (+)-03219A. Org. Lett 2021, 23, 2248–2252. [PubMed: 33635666] (c)Wai H; Koelblen T; Hayes ME; Burris TP; Micalizio GC Progress toward the De Novo Asymmetric Synthesis of Euphanes. Org. Lett 2022, 24, 3686–3690. [PubMed: 35584298] See also ref 14.

[13]. For related oxidative dearomatization followed by semi-Pinacol rearrangement: (a)Guérard KC; Guérinot A; Bouchard-Aubin C; Ménard M-A; Lepage M; Beaulieu MA; Canesi S Oxidative 1,2- and 1,3-Alkyl Shift Processes: Developments and Applications in Synthesis. J. Org. Chem 2012, 77, 2121–2133. [PubMed: 22332792] (b)Guérard KC; Sabot C; Beaulieu M-A; Giroux M-A; Canesi S 'Aromatic Ring Umpolung', a Rapid Access to the Main Core of Several Natural Products. Tetrahedron 2010, 66, 5893–5901.(c)Guérard KC; Chapelle C; Giroux M-A; Sabot C; Beaulieu M-A; Achache N; Canesi S An Unprecedented Oxidative Wagner–Meerwein Transposition. Org. Lett 2009,11, 4756–4759. [PubMed: 19769388]

[14]. (a)Micalizio GC; Mizoguchi H The Development of Alkoxide Directed Metallacycle-Mediated Annulative Cross-Coupling Chemistry. Isr. J. Chem 2017, 57, 228–238. [PubMed: 28652644] (b)Millham AB; Bhatt CP; Micalizio GC From Metallacycle-Mediated Annulative Cross-Coupling to Steroidal Tetracycles through Intramolecular C9–C10 Bond Formation. Org. Lett 2020, 22, 6595–6599. [PubMed: 32806140] (c)Nicholson JM; Millham AB; Bucknam AR; Markham LE; Sailors XE; Micalizio GC A General Enantioselective and Stereochemically Divergent Four-Stage Approach to Fused Tetracyclic Terpenoid Systems. J. Org. Chem. 2022, 87, 3352–3362. [PubMed: 35175755]

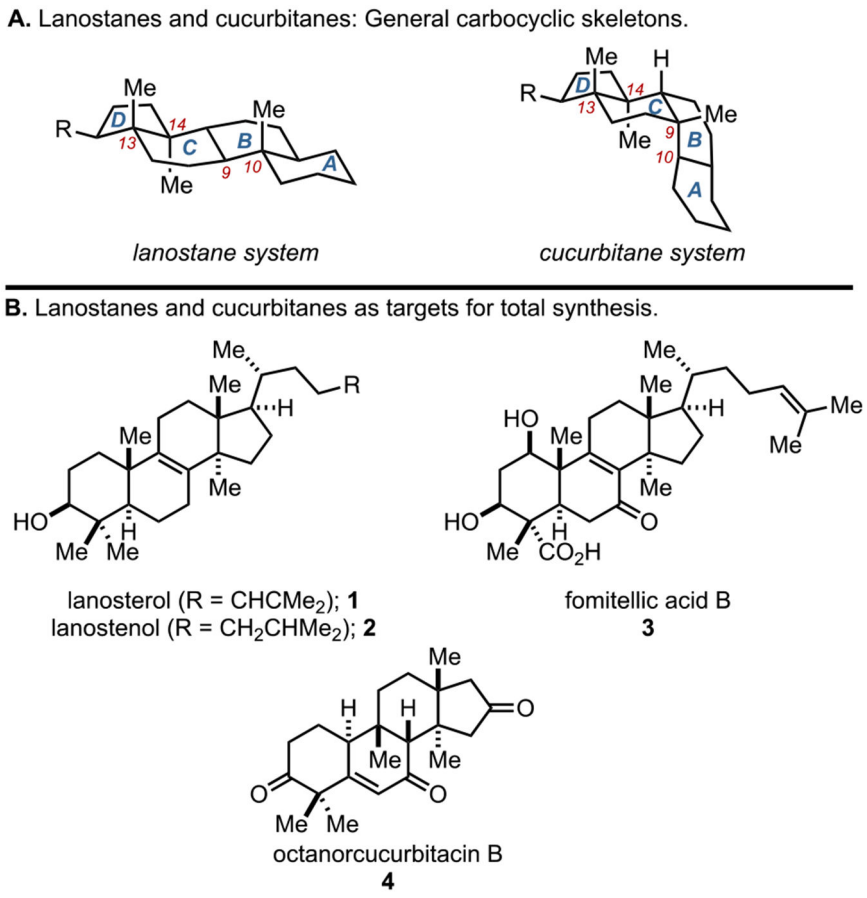

Figure 1.
Lanostanes and cucurbitanes as targets for total synthesis.

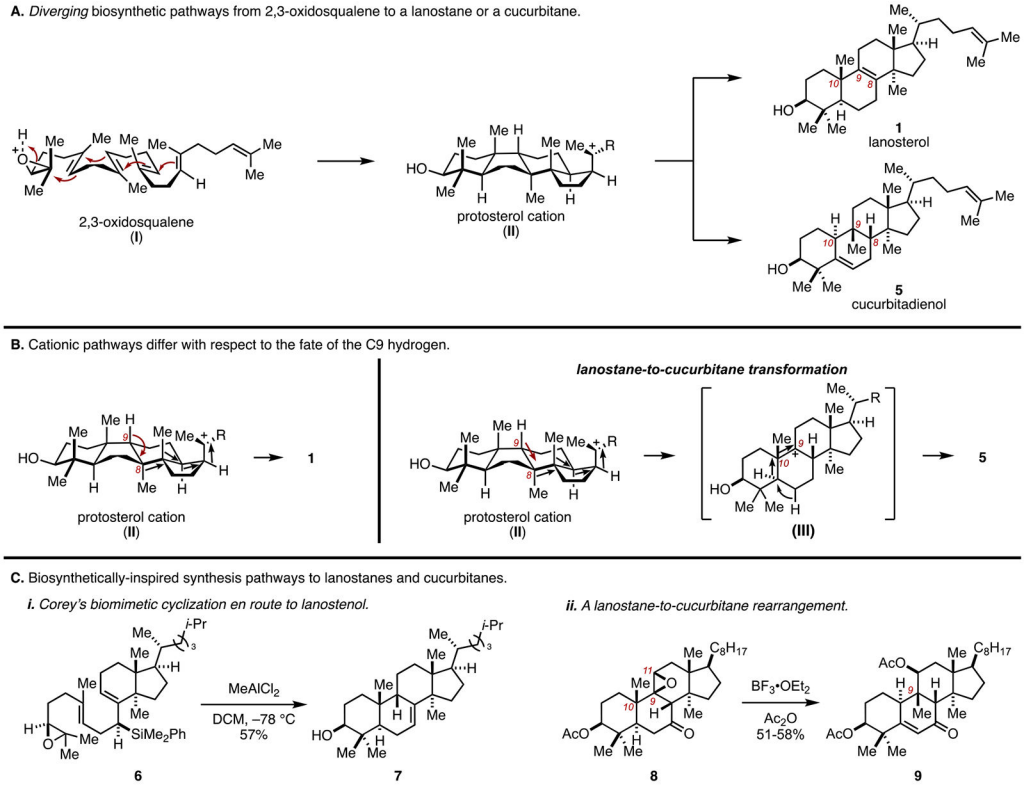

Figure 2.

Diverging biosynthetic pathways from the protosterol cation to lanostanes or cucurbitanes, and efforts to accomplish laboratory syntheses of such systems through bio-inspired cationic rearrangements.

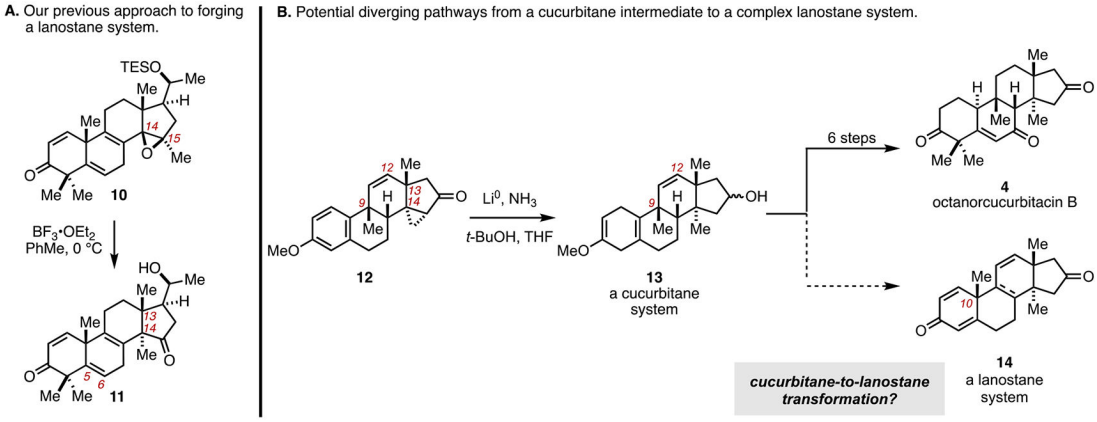

Figure 3.

Pursuit of a pathway from synthetic tetracycle **11** employed for the total synthesis of octanorcucurbitacin B (**12**), to a lanostane system by a novel cucurbitane-to-lanostane transform.

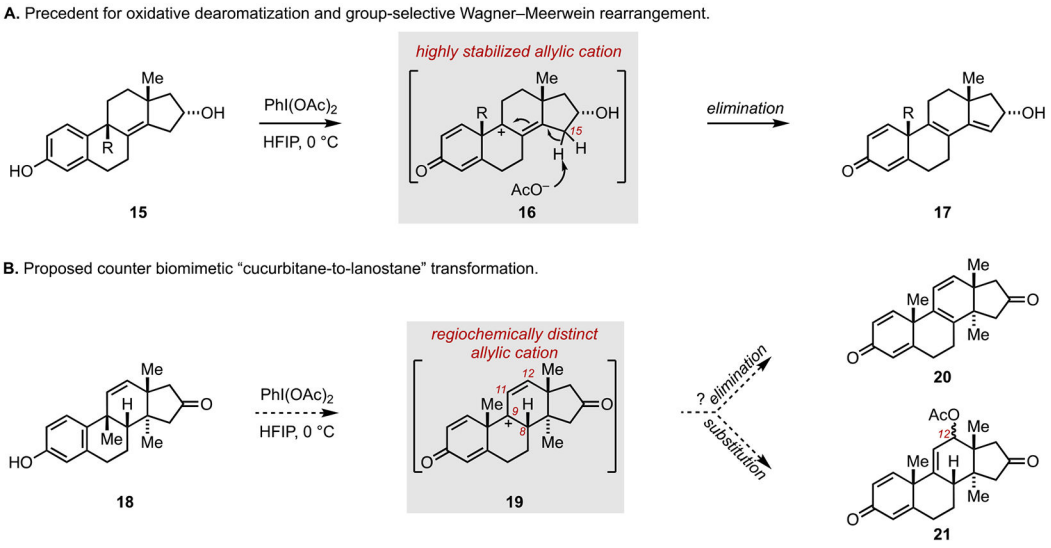

Figure 4.

Proposed counter biomimetic cucurbitane-to-lanostane transform via oxidative dearomatization and group selective Wagner–Meerwein rearrangement–Termination of the reaction cascade by elimination of substitution.

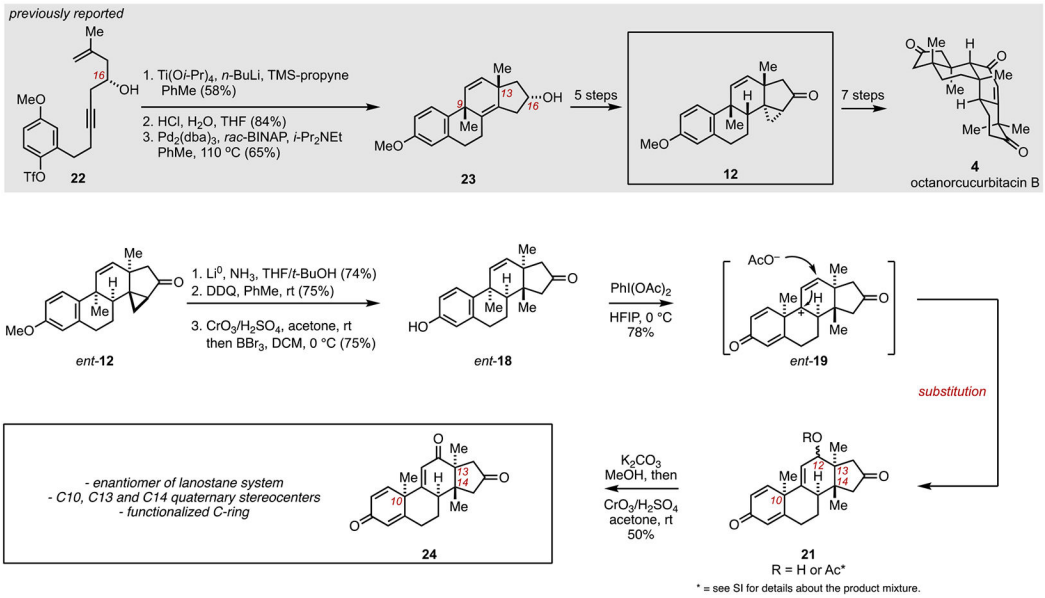

Figure 5.

Access to a C12 oxygenated lanostane system through oxidative dearomatization followed by group selective Wagner–Meerwein rearrangement and regioselective trapping of the resulting carbocation at C12.